ONCOLOGY

CrossMark

Evaluation of T categories for pure ground-glass nodules with semi-automatic volumetry: is mass a better predictor of invasive part size than other volumetric parameters?

Hyungjin Kim[1] · Jin Mo Goo[1,2] · Chang Min Park[1,2]

Abstract

Objectives This study aimed to investigate the diagnostic advantage of nodule mass in differentiating invasive pulmonary adenocarcinomas (IPAs) among pure ground-glass nodules (pGGNs) over other volumetric measurements. Another aim of this study was to analyse the correlation between volumetric measurements on computed tomography (CT) scans and the pathological invasive component size.

Methods This Institutional Review Board-approved retrospective study included 117 patients (men:women = 53:64; mean age, 57.3 years) with 117 pGGNs. Semi-automatic segmentation was performed for all nodules, and volumetric measurements, such as nodule volume, attenuation, mass, two-dimensional (2D) average diameter and three-dimensional (3D) longest diameter, were obtained. Receiver operating characteristic (ROC) curve analyses were performed to evaluate the diagnostic performances of the volumetric parameters in discriminating IPAs. Spearman correlation coefficients were calculated between the volumetric measurements and the invasive component size.

Results Area under the ROC curve for mass was 0.792 (95% CI, 0.691-0.872) in non-enhanced CT and 0.730 (95% CI, 0.607-0.832) in contrast-enhanced CT. Nodule mass was not superior to 2D average diameter for the differentiation of IPAs in both non-enhanced (0.792 vs 0.780; $p = 0.501$) CT and contrast-enhanced CT scans (0.730 vs 0.700; $p = 0.319$). The correlation between the volumetric measurements (mass, 3D longest diameter and 2D average diameter) and the invasive component size was moderate (Spearman's *rho*, 0.401-0.422) in non-enhanced CT and weak (Spearman's *rho*, 0.276-0.310) in contrast-enhanced CT.

Conclusions Nodule mass measurement had no strength over other volumetric parameters for the prediction of pathological invasiveness in the diagnosis of pGGNs.

Key Points

• *Mass is not superior to other volumetric measurements for the diagnosis of pure ground-glass nodules.*
• *Mass and two-dimensional average diameter exhibited comparable performance for the discrimination of invasive adenocarcinomas among pure ground-glass nodules.*
• *The diagnostic performance of volumetric measurements was lower on contrast-enhanced CT scans.*
• *The correlation between the volumetric measurements and the invasive component size was moderate on non-enhanced CT scans and weak on contrast-enhanced CT scans.*

✉ Jin Mo Goo
   jmgoo@plaza.snu.ac.kr

1   Department of Radiology, Seoul National University College of Medicine, and Institute of Radiation Medicine, Seoul National University Medical Research Center, 101, Daehak-ro, Jongno-gu, Seoul 03080, Korea

2   Cancer Research Institute, Seoul National University, 101, Daehak-ro, Jongno-gu, Seoul 03080, Korea

Abbreviations
IPA   Invasive pulmonary adenocarcinoma
pGGN   Pure ground-glass nodule
PSN   Part-solid nodule
SSN   Subsolid nodule

Introduction

International Association for the Study of Lung Cancer (IASLC) proposed the eighth edition of the clinical and patho-logical T descriptor classification of lung adenocarcinomas [1]. IASLC recommended the classification of cT according to the solid portion size on CT scans and the determination of pT according to the histopathological invasive part size [1]. For the part-solid nodules (PSNs), several studies have shown that the solid portions in PSNs are well correlated to the invasive component of the pathological specimens [2–4]. However, for the pure ground-glass nodules (pGGNs), which do not have any measurable solid portion on CT scans, 'cTis' should be assigned to all pGGNs of total size ranging from 0.6 to 3.0 cm [1].

Nevertheless, it is well known that a subset of pGGNs exhibits a pathological invasive component [5]. Moon et al. [6] reported that 20.5% of the pGGNs in their study were invasive pulmonary adenocarcinomas (IPAs), and Lim et al. [7] stated that 39% of the pGGNs ≥10 mm in diameter were IPAs. In the absence of a measurable solid portion, researchers have searched for other potential sur-rogates including nodule size, volume, mass, histogram features or texture features which could be used to predict IPAs appearing as pGGNs [5–11].

Among those tentative surrogates, nodule mass was re-ported as a less variable parameter than nodule volume. It was also reported that the mass could reflect the change in volume and attenuation simultaneously, given that it is cal-culated as the product of volume and attenuation [12]. Nonetheless, the usefulness of nodule mass among pGGNs for the differentiation of IPAs and its potential as a surrogate for the pathological invasive component have not been in-vestigated thoroughly [7, 10]. The strength of mass over other size metrics in the diagnosis of pGGNs has not yet been established.

Therefore, we aimed to investigate the diagnostic advan-tage of mass in differentiating IPAs among pGGNs over other volumetric measurements on both non-enhanced and contrast-enhanced CT scans. We also analysed the correlation between the volumetric measurements including mass and the patho-logical invasive component size on surgical specimens.

Materials and methods

This retrospective analysis was approved by the Institutional Review Board of Seoul National University Hospital, and the requirement of written informed consent was waived.

Study population

Patients who had pGGNs at the preoperative chest CT scans and subsequently underwent surgical resections at our hospital between November 2011 and July 2017 were retrospectively identified from the electronic medical records by a board-certified thoracic radiologist (H.K. with 7 years of experience in CT imaging). Among 124 patients, 7 patients (5.6%) were excluded because of semi-automatic nodule segmentation fail-ure. Consequently, a total of 117 patients, 53 men and 64 wom-en, were included in this study. The mean age (± standard deviation) of the overall population was 57.3 ± 11.1 years (men, 58.4 ± 11.7 years; women, 56.3 ± 10.6 years; $p = 0.311$).
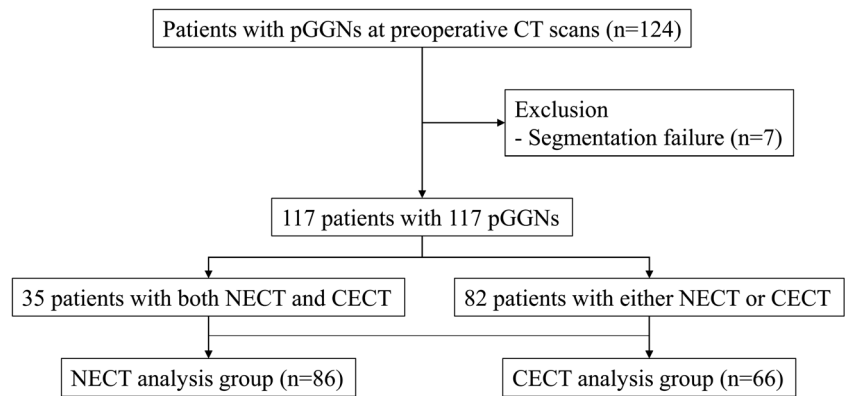
A single nodule was selected from each patient. A dominant lesion was chosen for patients with multiple resected pGGNs. Among 117 patients, 35 patients had both non-enhanced and contrast-enhanced CT scans; the rest of the population ($n = 82$) had either non-enhanced ($n = 51$) or contrast-enhanced CT scans ($n = 31$) (Fig. 1). The median interval between CT and surgical resection was 2 days [interquartile range (IQR), 1-23 days]. Sixty-six nodules (56.4%) were located in the upper lobes. For the surgical methods, lobectomy was performed in 23 patients, segmentectomy in 33 patients and wedge resection in 61 patients. Pathology revealed that there were 14 atypical adenomatous hyperplasias (AAHs), 35 adenocarcinomas in situ (AISs), 34 minimally invasive adenocarcinomas (MIAs) and 34 IPAs. The median invasive component size was 2 mm (IQR, 2-3 mm) in MIAs ($n = 31$; measurements were not available in 3 patients) and was 6 mm (IQR, 6-8 mm) in IPAs ($n = 11$; mea-surements were not available in 23 patients).

Part of the study population was reported in past studies [13–17]. However, none of those studies focused on the dif-ferentiation of pGGNs, and the topics were completely differ-ent from that of the present study.

CT acquisition

CT scans were performed with seven different scanners from three manufacturers (Brilliance 64, Ingenuity, iCT and iQon, Philips Healthcare, Best, The Netherlands; Discovery CT750HD, GE Healthcare, Waukesha, WI, USA; Sensation 16 and Definition, Siemens Healthcare, Forchheim, Germany). Our hospital is a tertiary medical centre, and it

Patients with pGGNs at preoperative CT scans (n=124)

Exclusion
- Segmentation failure (n=7)

117 patients with 117 pGGNs

35 patients with both NECT and CECT

82 patients with either NECT or CECT

NECT analysis group (n=86)

CECT analysis group (n=66)

operates multiple CT scanners from various vendors. Thus, heterogeneity in imaging acquisition was inevitable during the retrospective data collection. All patients underwent CT scans from the lung apex to base at suspended maximum inspiration. Scans were performed with 120 kVp and mAs ranging approximately from 20 to 200 mAs with or without automatic exposure control of each vendor. It is noteworthy that all CT scans were reconstructed with slice thickness/ interval of 0.625, 1 or 1.25 mm to assure adequate volumetry analysis. Lung kernel or sharp kernel was used for the reconstruction. For contrast enhancement, a total of 70-90 mL of 370 mgI/mL of the contrast material, most of which was iopamidol (Pamiray 370; Dongkook Pharmaceutical, Seoul, Korea) or iopromide (Ultravist 370; Schering, Berlin, Germany), was injected at a rate of 2.0-2.3 mL/s using a power injector. CT scanning was performed with a 60-s delay.

CT image analysis

All image analysis was performed by a single radiologist (H.K.) with commercial software (AVIEW, Coreline Soft, Seoul, Korea). This software enables semi-automatic segmentation of nodules in two steps. The reader determined the target by dragging a line traversing the nodule on an axial plane and then selected the nodule type (pGGN). Then, the software automatically defined the nodule margin, calculated the volumetric profiles, and provided quantitative measurements. The reader was allowed to adjust the nodule margin in cases of suboptimal segmentation by tuning two segmentation parameters: nodule shape and attenuation threshold. In our study, nodule segmentation was evaluated subjectively, and segmentation success was defined as correct segmentation proportion of 80% or greater, according to past literature [13, 14, 18]. Volumetric features of nodule volume, attenuation, mass, two-dimensional (2D) average diameter and three-dimensional (3D) longest diameter were obtained. Mass was calculated as follows.

$$\text{Mass} = \text{Volume} \times [(\text{Attenuation} + 1,000) \times 0.001]$$

Pathological diagnosis

In our institution, all surgical specimens containing subsolid nodules (SSNs) were fixed by infusing 10% buffered formalin through the transpleural and transbronchial approach to produce an inflated state and precisely measure the invasive adenocarcinoma component [2]. Haematoxylin and eosin were used for staining the specimens. All pathological diagnoses were established based on the surgical specimens by attending pulmonary pathologists of Seoul National University Hospital according to the 2011 IASLC/ American Thoracic Society (ATS)/ European Respiratory Society (ERS) pulmonary adenocarcinoma classification [19]. Pathological diagnosis and invasive component size of each nodule were recorded [19]. The invasive component size was recorded only for pT1mi and pT1a according to our institutional protocol.

Statistical analysis

We calculated descriptive statistics of the volumetric features according to the pathologic diagnosis. After testing the normality of variables using Shapiro-Wilk test, values were described with either median (IQR) or mean ± standard deviation. Then, the features between preinvasive lesions/MIAs and IPAs were compared. Independent *t*-test or Mann-Whitney *U* test was used for the continuous variables (age, 3D longest diameter, 2D average diameter, volume, attenuation, and mass), and chi-squared test was used for the categorical variable (sex). Subsequently, receiver operating characteristic (ROC) curve analysis was performed to evaluate the diagnostic performance of each volumetric feature in discriminating IPAs. Areas under the ROC curve (AUCs) were obtained and compared between the features using DeLong et al.'s method [20]. For multiple comparisons, Bonferroni correction was applied to minimise α (type I error). Therefore, the significance level was adjusted to 0.01 for comparisons of volumetric features between preinvasive lesions/MIAs and IPAs and 0.0125 for comparisons of AUCs between mass and the other four volumetric features.

To analyse the correlation between the invasive component size of the surgical specimens and the volumetric features obtained from the semi-automated volumetry, Spearman's rank correlation coefficient (*rho*) was calculated with 95% confidence interval (CI). Correlation coefficient between 0.0-0.2 was regarded as negligible, 0.2-0.4 as weak, 0.4-0.7 moderate, 0.7-0.9 strong and 0.9-1.0 very strong correlation [21].

All analyses were conducted for patients who underwent non-enhanced CT scans and those who had contrast-enhanced CT scans, respectively, to exclude bias caused by the contrast enhancement. A subset of patients ($n = 35$) who had both non-enhanced and enhanced CT scans belonged to both analysis groups. All statistical analyses were performed using two commercial software programs (MedCalc version 12.3.0, MedCalc Software, Mariakerke, Belgium and SPSS 19.0, IBM SPSS Statistics, Armonk, NY, USA). A *p* value <0.05 was considered as statistically significant.

Results

Volumetric measurements on non-enhanced CT scans and pathological diagnosis

Descriptive statistics of the volumetric features for each pathological diagnosis are shown in Table 1. All volumetric features exhibited an increasing trend according to the pathologic disease spectrum from AAH to IPA.

There were significant differences between the preinvasive lesions/MIAs and IPAs for all volumetric features (all $p <$ 0.001) (Electronic Supplementary Table 1). ROC analysis for differentiating IPAs among pGGNs demonstrated that AUC was highest for mass (0.792; 95% CI, 0.691-0.872) and lowest for 3D longest diameter (0.739; 95% CI, 0.634-0.828) (Table 2). For the pairwise comparisons of AUCs between mass and the other four volumetric features, mass was

superior to 3D longest diameter ($p = 0.009$) and volume (0.747; $p < 0.001$). However, AUCs were not significantly different between mass and 2D average diameter (0.780; $p = 0.501$) and between mass and attenuation (0.752; $p = 0.598$).

Volumetric measurements of contrast-enhanced CT scans and pathological diagnosis

Table 3 shows descriptive statistics of the volumetric features for each pathological diagnosis. All volumetric features showed increasing tendency from AAH to IPA according to the pathological disease spectrum.

There were significant differences between the preinvasive lesions/MIAs and IPAs for attenuation ($p = 0.002$) and mass ($p = 0.005$) (Electronic Supplementary Table 2). Two-dimensional average diameter showed marginal statistical significance ($p = 0.010$). Three-dimensional longest diameter ($p = 0.029$) and volume ($p = 0.025$) were not significantly different for the preinvasive lesions/MIAs and IPAs after adjustment of the statistical significance level for the multiple comparisons. ROC analysis for differentiating IPAs among pGGNs demonstrated that AUC was highest for attenuation (0.761; 95% CI, 0.640-0.857) and lowest for 3D longest diameter (0.679; 95% CI, 0.553-0.789) (Table 4). AUC for mass was 0.730 (95% CI, 0.607-0.832). For the pairwise comparisons of AUCs, there were no significant differences between mass and the other four volumetric parameters [$p = 0.067$ between mass and 3D longest diameter; $p = 0.319$ between mass and 2D average diameter (AUC, 0.700); $p = 0.015$ between mass and volume (AUC, 0.683); $p = 0.749$ between mass and attenuation] (Fig. 2).

Correlation between volumetric features of non-enhanced CT and invasive component size

Invasive component size was recorded in a subset of patients ($n = 66$); median invasive component size was 1 mm (IQR, 0-3

Table 1 Volumetric measurements of pure ground-glass nodules on non-enhanced CT scans according to the pathological diagnosis

	AAH ($n = 8$)	AIS ($n = 21$)	MIA ($n = 30$)	IPA ($n = 27$)
Age (years)	54 (43-63)	61 (51-64)	57 (52-62)	61 (48-71)
Sex (M:F)a	1:7	11:10	15:15	14:13
3D longest diameter (mm)	9.1 (8.3-10.1)	12.1 (8.9-14.0)	14.4 (9.2-19.1)	15.7 (14.3-21.3)
2D average diameter (mm)	7.0 (6.6- 8.7)	8.5 (7.6-10.5)	10.5 (7.8-13.6)	12.8 (10.8-14.9)
Volume (mm^3)	186.1 (134.7-339.5)	452.1 (211.4-578.1)	625.2 (271.4-1,258.1)	951.7 (640.3-1,682.3)
Attenuation (HU)b	-670.8 ± 79.4	-641.7 ± 83.8	-647.3 ± 68.6	-581.5 ± 72.0
Mass (g)	0.06 (0.04-0.13)	0.13 (0.08-0.22)	0.18 (0.09-0.45)	0.40 (0.27-0.79)

Unless otherwise specified, data are median (with interquartile range *in parentheses*)

[a] Data are numbers of patients

[b] Data are mean ± standard deviation

AAH atypical adenomatous hyperplasia, *AIS* adenocarcinoma in situ, *HU* Hounsfield units, *IPA* invasive pulmonary adenocarcinoma, *MIA* minimally invasive adenocarcinoma

Table 2 ROC analysis of the volumetric measurements to discriminate IPAs among pure ground-glass nodules on non-enhanced CT scans

	AUC	95% CI	*p* value	Threshold[a]	Sensitivity (%)	Specificity (%)
3D longest diameter	0.739	0.634-0.828	<0.001	13.9 mm	85.2	61.0
2D average diameter	0.780	0.678-0.862	<0.001	10.4 mm	85.2	64.4
Volume	0.747	0.642-0.835	<0.001	531.9 mm^3	81.5	62.7
Attenuation	0.752	0.647-0.839	<0.001	-675 HU	96.3	42.4
Mass	0.792	0.691-0.872	<0.001	0.23 g	81.5	67.8

AUC area under the receiver operating characteristic curve, *CI* confidence interval, *HU* Hounsfield units, *IPA* invasive pulmonary adenocarcinoma, *ROC* receiver operating characteristics

[a] Optimal threshold was calculated based on the Youden index

mm). The correlations between the volumetric features and the pathological invasive component size were significant for 3D longest diameter ($p < 0.001$; $rho = 0.422$; moderate), 2D average diameter ($p = 0.001$; $rho = 0.401$; moderate), volume ($p = 0.002$; $rho = 0.375$; weak) and mass ($p = 0.001$; $rho = 0.410$; moderate) (Electronic Supplementary Table 3). Attenuation had no significant correlation with invasive component size ($p = 0.176$; $rho = 0.168$; negligible).

Correlation between volumetric features of contrast-enhanced CT and invasive component size

Invasive component size was obtained in a subset of the study population ($n = 54$). Median invasive component size was 1 mm (IQR, 0-3 mm). The correlations between volumetric features and pathological invasive component size were significant for 3D longest diameter ($p = 0.022$; $rho = 0.310$; weak), 2D average diameter ($p = 0.044$; $rho = 0.276$; weak), volume ($p = 0.039$; $rho = 0.281$; weak) and mass ($p = 0.035$; $rho = 0.287$; weak) (Electronic Supplementary Table 4). Attenuation did not exhibit a significant correlation with invasive component size ($p = 0.394$; $rho = 0.118$; negligible).

Discussion

In this study, we demonstrated that nodule mass is not superior to other volumetric measurements, such as 2D average diameter, for the discrimination of IPAs manifesting as pGGNs. The correlation between the volumetric measurements (mass, 3D longest diameter and 2D average diameter) and the invasive component size was moderate on non-enhanced CT scans and weak on contrast-enhanced CT scans.

The advantages of volumetric measurements for lung nodules have repeatedly been reported in the literature regarding measurement accuracy [22–24] and reproducibility [25–27]. The feasibility of volumetric analysis for the SSNs has also been assessed in the past decade, and a few studies reported the practicability and suggested the measurement variability ranges for the volume and mass [28–30]. Furthermore, Kim et al. [16] recently reported that the effective diameter obtained from semi-automatic volumetry exhibited higher diagnostic accuracy and reproducibility between readers for the differentiation of IPAs among SSNs than manual average diameter measurements. In this circumstance, it is assumed that the volumetric approach is a convincing diagnostic option for the SSNs. Among multiple volumetric measurements obtainable from the semi-automatic

Table 3 Volumetric measurements of pure ground-glass nodules on contrast-enhanced CT scans according to the pathological diagnosis

	AAH ($n = 10$)	AIS ($n = 17$)	MIA ($n = 22$)	IPA ($n = 17$)
Age (years)	56 (53, 67)	58 (51, 66)	57 (55, 66)	63 (50, 67)
Sex (M:F)a	2:8	5:12	12:10	9:8
3D longest diameter (mm)	8.6 (7.5-12.4)	14.1 (11.1-17.1)	14.7 (11.2-19.8)	16.6 (13.9-20.8)
2D average diameter (mm)b	8.2 ± 2.1	10.9 ± 3.5	11.3 ± 4.6	13.6 ± 4.5
Volume (mm^3)	223.8 (145.5-606.9)	618.3 (294.1-1,387.0)	803.4 (371.7-1,631.5)	1,055.3 (660.2-1,555.4)
Attenuation (HU)b	-626.3 ± 116.0	-621.8 ± 73.1	-626.6 ± 73.0	-549.2 ± 80.0
Mass (g)	0.09 (0.04-0.23)	0.23 (0.13-0.54)	0.29 (0.12-0.61)	0.44 (0.32-0.83)

Unless otherwise specified, data are median (with interquartile range *in parentheses*)

AAH atypical adenomatous hyperplasia, *AIS* adenocarcinoma in situ, *HU* Hounsfield units, *IPA* invasive pulmonary adenocarcinoma, *MIA* minimally invasive adenocarcinoma

[a] Data are numbers of patients

[b] Data are mean ± standard deviation

Table 4 ROC analysis of the volumetric measurements to discriminate IPAs among pure ground-glass nodules on contrast-enhanced CT scans

	AUC	95% CI	*p* value	Threshold[a]	Sensitivity (%)	Specificity (%)
3D longest diameter	0.679	0.553-0.789	0.013	14.4 mm	76.5	59.2
2D average diameter	0.700	0.575-0.807	0.004	9.8 mm	88.2	49.0
Volume	0.683	0.557-0.792	0.010	820.2 mm^3	76.5	67.3
Attenuation	0.761	0.640-0.857	<0.001	-536 HU	58.8	87.8
Mass	0.730	0.607-0.832	0.001	0.37 g	76.5	67.3

AUC area under the receiver operating characteristic curve, *CI* confidence interval, *HU* Hounsfield units, *IPA* invasive pulmonary adenocarcinoma, *ROC* receiver operating characteristics

[a] Optimal threshold was calculated based on the Youden index

segmentation, mass was suggested as a less variable [12] and useful parameter for the evaluation of SSNs [7, 10]. This is particularly interesting for the pGGNs as they do not have a measurable solid portion which is a direct indicator of pathological invasiveness. Nevertheless, the diagnostic performance of the nodule mass was not superior to 2D average diameter as analysed in the present study.

The current standard for the measurement of SSNs uses the average diameter, which is measured manually with an electronic calliper on thin-section CT scans [31, 32]. Although manual measurement was not analysed in our study, we revealed that there are no significant differences in the diagnostic capability between 2D average diameter on an axial image and nodule mass at both non-enhanced and contrast-enhanced CT scans. Considering that nodule mass is affected by contrast material injection and the threshold for the diagnosis should thus be changed according to the enhancement status as demonstrated in our study (i.e. 0.23 g in non-enhanced CT and 0.37 g in contrast-enhanced CT; 61% increase in enhanced CT), it would be more practical and easy to use a single threshold of 2D

average diameter (i.e. 10 mm; sensitivity 85.2% and specificity 64.4% at non-enhanced CT; sensitivity 88.2% and specificity 49.0% at enhanced CT), which can be applied regardless of the enhancement status. In fact, the contrast-enhancement profile of a nodule is influenced by the patient factor, contrast medium factor and CT scanning factor [33]. Therefore, mass, which reflects nodule attenuation, is inherently a vulnerable parameter for the acquisition setting. Thus, we cautiously suggest that the evaluation of pGGNs based on the 2D average diameter is sufficient and practical for clinical practice.

Recently, Heidinger et al. [8] reported a similar finding that measuring nodule volume and attenuation of pGGNs had no advantage over average diameter measurement. They performed correlation analysis between the CT measurements and the invasive foci (size and number) [8]. The results were similar to those in our study, and the correlation coefficients were 0.417 between the average diameter and the invasive focus, 0.401 between the nodule volume and the invasive focus, and 0.237 between the mean density and the invasive focus [8]. However, the diagnostic performance of the quantitative
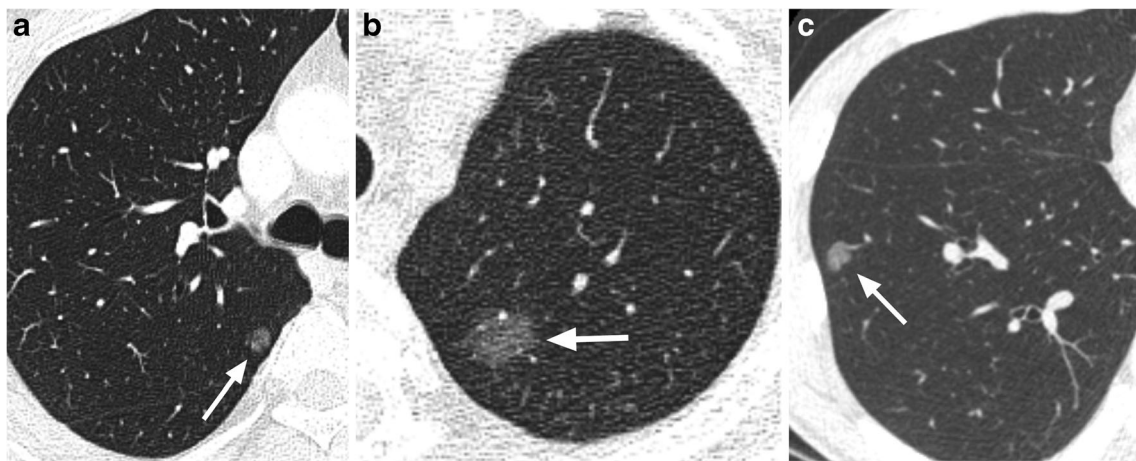

Fig. 2 Representative cases of pure ground-glass nodules. **a** Adenocarcinoma-in-situ in a 42-year-old man. Two-dimensional average diameter was 7.6 mm, and nodule mass was 0.11 g (contrast-enhanced CT). Both measurements corresponded well with the diagnosis. **b** Adenocarcinoma-in-situ in a 47-year-old man. The two-dimensional average diameter was 13.3 mm, and nodule mass was 0.49 g (non-enhanced CT). Based on the volumetric measurements, invasive adenocarcinoma was more likely than a preinvasive lesion. **c** Adenocarcinoma in a 45-year-old male. Two-dimensional average diameter was 9.2 mm, and nodule mass was 0.17 g (non-enhanced CT). Volumetric measurements, which are suggestive of a preinvasive lesion, were discordant with the diagnosis. Invasive component size was 6 mm in this lesion

features for identifying IPAs was not evaluated, and the nodule mass was not calculated in their study. Also, the correlation analysis cannot be directly translated into a classification (differentiation) task. Thus, in this respect, we believe that our study provided additional supporting evidence for the usage of the conventional measurement metric, average diameter, rather than mass or volume for pGGNs.

Interestingly, the diagnostic performance of volumetric measurements and the correlation between the CT measurements and the invasive component size were lower at contrast-enhanced CT scans. This is plausible given that any penetrating or abutting vessels to the nodule may increase the nodule attenuation and size as well as nodule volume substantially [14]. The software we used in the present study applied a vessel removal algorithm to solve this issue but the measurements led to the suboptimal results. Cohen et al. [14] previously reported that the volumetric parameters of PSNs, including diameter and volume, significantly increased in enhanced CT. Although pGGNs were not analysed in that study, similar results may be inferred for the pGGNs.

Lastly, 10 out of 117 pGGNs (8.5%) had an invasive component size larger than 10 mm (data not shown). In our institution, an invasive component size larger than 10 mm is described with a greater than symbol (>10 mm) in the pathology report and the precise size is not measured. Thus, these nodules were excluded from the correlation analysis in our study. Weak-to-moderate correlation between the invasive component size and the volumetric measurements might be partly attributed to the exclusion of these nodules. A narrow range of variables may result in small correlation coefficients [34]. Nevertheless, it is noteworthy that a subset of pGGNs may have a substantially large invasive component. The median average diameter of these nodules was 13.9 mm (IQR, 13.2-17.5 mm).

There were several limitations to this study. First, the CT scans included in our study had heterogeneous acquisition settings including various manufacturers. Our hospital is a tertiary medical centre, which operates a few different CT scanners. Thus, this was an inevitable limitation of this retrospective study's design. Second, one commercial software was used, and our study results might be software specific. In addition, this software requires further validation for the solid nodules as well as SSNs. Third, manual measurements were not performed for the nodules. We focused on semi-automated volumetric measurements as the nodule mass cannot be accurately assessed with manual measurements. Comparison of the volumetric parameters, including mass with manual average diameter in terms of the diagnostic performance and reproducibility, is warranted. Fourth, measurement variability was not analysed. The inter- and intra-reader agreements of the software measurements for SSNs were excellent (intra-class correlation coefficient, 0.90-0.98) according to our prior study [35]. Fifth, our study population comprised patients who underwent surgical resection, and this might have induced selection bias. Small indolent pGGNs, which are usually followed-up with serial CT scans, were not analysed. Thus, the invasive component size in this study may not accurately represent that in screening-detected or incidentally detected pGGNs. Lastly, findings in this retrospective observational study should be validated in a future prospective cohort.

In conclusion, nodule mass measurement had no strength over other volumetric parameters for the prediction of invasiveness of lung adenocarcinoma in pGGNs. There was a moderate correlation between the volumetric parameters and the pathological invasive component.

Compliance with ethical standards

Guarantor The scientific guarantor of this publication is Jin Mo Goo.

Conflict of interest The authors of this manuscript declare no relationships with any companies, whose products or services may be related to the subject matter of the article.

Statistics and biometry No complex statistical methods were necessary for this paper.

Informed consent Written informed consent was waived by the Institutional Review Board.

Ethical approval Institutional Review Board approval was obtained.

Study subjects or cohorts overlap Some study subjects or cohorts have been previously reported in journal articles (Eur Radiol 2016, 26:4465-4474; Eur J Radiol 2016, 85:1174-1180; Eur Radiol 2017, 27:3266-3274; Eur Radiol 2017, doi:10.1007/s00330-017-5171-7; Eur Radiol 2017, 27:1369-1376).

Methodology

- retrospective
- diagnostic or prognostic study
- performed at one institution

References

1. Travis WD, Asamura H, Bankier AA et al (2016) The IASLC Lung Cancer Staging Project: proposals for coding T categories for subsolid nodules and assessment of tumor size in part-solid tumors in the forthcoming eighth edition of the TNM classification of lung cancer. J Thorac Oncol 11:1204–1223
2. Lee KH, Goo JM, Park SJ et al (2014) Correlation between the size of the solid component on thin-section CT and the invasive component on pathology in small lung adenocarcinomas manifesting as ground-glass nodules. J Thorac Oncol 9:74–82
3. Ko JP, Suh J, Ibidapo O et al (2016) Lung adenocarcinoma: correlation of quantitative CT findings with pathologic findings. Radiology 280:931–939

4. Yanagawa M, Johkoh T, Noguchi M et al (2017) Radiological prediction of tumor invasiveness of lung adenocarcinoma on thin-section CT. Medicine (Baltimore) 96:e6331

5. Lee SM, Park CM, Goo JM, Lee HJ, Wi JY, Kang CH (2013) Invasive pulmonary adenocarcinomas versus preinvasive lesions appearing as ground-glass nodules: differentiation by using CT features. Radiology 268:265–273

6. Moon Y, Sung SW, Lee KY, Sim SB, Park JK (2016) Pure ground-glass opacity on chest computed tomography: predictive factors for invasive adenocarcinoma. J Thorac Dis 8:1561–1570

7. Lim HJ, Ahn S, Lee KS et al (2013) Persistent pure ground-glass opacity lung nodules ≥10 mm in diameter at CT scan: histopathologic comparisons and prognostic implications. Chest 144:1291–1299

8. Heidinger BH, Anderson KR, Nemec U et al (2017) Lung adenocarcinoma manifesting as pure ground-glass nodules: correlating CT size, volume, density, and roundness with histopathologic invasion and size. J Thorac Oncol 12:1288–1298

9. Ding H, Shi J, Zhou X et al (2017) Value of CT characteristics in predicting invasiveness of adenocarcinoma presented as pulmonary ground-glass nodules. Thorac Cardiovasc Surg 65:136–141

10. Hwang IP, Park CM, Park SJ et al (2015) Persistent pure ground-glass nodules larger than 5 mm: differentiation of invasive pulmonary adenocarcinomas from preinvasive lesions or minimally invasive adenocarcinomas using texture analysis. Invest Radiol 50:798–804

11. Li Q, Fan L, Cao ET, Li QC, Gu YF, Liu SY (2017) Quantitative CT analysis of pulmonary pure ground-glass nodule predicts histological invasiveness. Eur J Radiol 89:67–71

12. de Hoop B, Gietema H, van de Vorst S, Murphy K, van Klaveren RJ, Prokop M (2010) Pulmonary ground-glass nodules: increase in mass as an early indicator of growth. Radiology 255:199–206

13. Cohen JG, Goo JM, Yoo RE et al (2016) Software performance in segmenting ground-glass and solid components of subsolid nodules in pulmonary adenocarcinomas. Eur Radiol 26:4465–4474

14. Cohen JG, Goo JM, Yoo RE et al (2016) The effect of late-phase contrast enhancement on semi-automatic software measurements of CT attenuation and volume of part-solid nodules in lung adenocarcinomas. Eur J Radiol 85:1174–1180

15. Cohen JG, Kim H, Park SB et al (2017) Comparison of the effects of model-based iterative reconstruction and filtered back projection algorithms on software measurements in pulmonary subsolid nodules. Eur Radiol 27:3266–3274

16. Kim H, Park CM, Hwang EJ, Ahn SY, Goo JM (2017) Pulmonary subsolid nodules: value of semi-automatic measurement in diagnostic accuracy, diagnostic reproducibility and nodule classification agreement. Eur Radiol. https://doi.org/10.1007/s00330-017-5171-7

17. Yoo RE, Goo JM, Hwang EJ et al (2017) Retrospective assessment of interobserver agreement and accuracy in classifications and measurements in subsolid nodules with solid components less than 8mm: which window setting is better? Eur Radiol 27:1369–1376

18. de Hoop B, Gietema H, van Ginneken B, Zanen P, Groenewegen G, Prokop M (2009) A comparison of six software packages for evaluation of solid lung nodules using semi-automated volumetry: what is the minimum increase in size to detect growth in repeated CT examinations. Eur Radiol 19:800–808

19. Travis WD, Brambilla E, Noguchi M et al (2011) International Association for the Study of Lung Cancer/American Thoracic Society/European Respiratory Society international multidisciplinary classification of lung adenocarcinoma. J Thorac Oncol 6:244–285

20. DeLong ER, DeLong DM, Clarke-Pearson DL (1988) Comparing the areas under two or more correlated receiver operating characteristic curves: a nonparametric approach. Biometrics 44:837–845

21. Karlik SJ (2003) Exploring and summarizing radiologic data. AJR Am J Roentgenol 180:47–54

22. Das M, Ley-Zaporozhan J, Gietema HA et al (2007) Accuracy of automated volumetry of pulmonary nodules across different multi-slice CT scanners. Eur Radiol 17:1979–1984

23. Das M, Muhlenbruch G, Katoh M et al (2007) Automated volumetry of solid pulmonary nodules in a phantom: accuracy across different CT scanner technologies. Invest Radiol 42:297–302

24. Doo KW, Kang EY, Yong HS, Woo OH, Lee KY, Oh YW (2014) Accuracy of lung nodule volumetry in low-dose CT with iterative reconstruction: an anthropomorphic thoracic phantom study. Br J Radiol 87:20130644

25. Gietema HA, Wang Y, Xu D et al (2006) Pulmonary nodules detected at lung cancer screening: interobserver variability of semiautomated volume measurements. Radiology 241:251–257

26. Goodman LR, Gulsun M, Washington L, Nagy PG, Piacsek KL (2006) Inherent variability of CT lung nodule measurements in vivo using semiautomated volumetric measurements. AJR Am J Roentgenol 186:989–994

27. Revel MP, Lefort C, Bissery A et al (2004) Pulmonary nodules: preliminary experience with three-dimensional evaluation. Radiology 231:459–466

28. Kim H, Park CM, Woo S et al (2013) Pure and part-solid pulmonary ground-glass nodules: measurement variability of volume and mass in nodules with a solid portion less than or equal to 5 mm. Radiology 269:585–593

29. Scholten ET, de Hoop B, Jacobs C et al (2013) Semi-automatic quantification of subsolid pulmonary nodules: comparison with manual measurements. PLoS One 8:e80249

30. Scholten ET, de Jong PA, Jacobs C et al (2015) Interscan variation of semi-automated volumetry of subsolid pulmonary nodules. Eur Radiol 25:1040–1047

31. Bankier AA, MacMahon H, Goo JM, Rubin GD, Schaefer-Prokop CM, Naidich DP (2017) Recommendations for measuring pulmonary nodules at CT: a statement from the Fleischner Society. Radiology 285:584–600

32. MacMahon H, Naidich DP, Goo JM et al (2017) Guidelines for management of incidental pulmonary nodules detected on CT images: from the Fleischner society 2017. Radiology 284:228–243

33. Bae KT (2010) Intravenous contrast medium administration and scan timing at CT: considerations and approaches. Radiology 256: 32–61

34. McDonald JH (2014) Handbook of biological statistics, 3rd edn. Sparky House Publishing, Baltimore

35. Garzelli L, Goo JM, Ahn SY et al (2018) Improving the prediction of lung adenocarcinoma invasive component on CT: value of a vessel removal algorithm during software segmentation of subsolid nodules. Eur J Radiol 100:58–65